Biophysical Chemistry 190–191 (2014) 32–40

Contents lists available at ScienceDirect

Biophysical Chemistry

journal homepage: http://www.elsevier.com/locate/biophyschem

Human neutrophil peptide 1 variants bearing arginine modified cationic side chains: Effects on membrane partitioning

Alessio Bonucci [a], Enrico Balducci [b], Manuele Martinelli [c], Rebecca Pogni [a,*]

[a] Department of Biotechnology, Chemistry and Pharmacy, University of Siena, 53100 Siena, Italy
[b] School of Biosciences and Biotechnologies, University of Camerino, 62032 Camerino, Italy
[c] Novartis Vaccines & Diagnostics, via Fiorentina 1, 53100 Siena, Italy

HIGHLIGHTS

- HNP-1 variants bearing Arginine modified side chains
- Model membranes mimicking composition of Gram-negative bacteria inner membrane
- Reduced interaction with negative charged model membranes
- Role of the Arg14 guanidino group for lipid interaction
- Comparison with native HNP-1 peptide at different peptide:lipid molar ratios

GRAPHICAL ABSTRACT

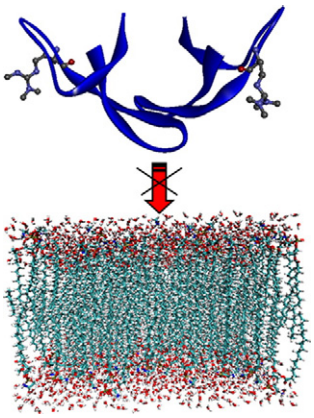

ARTICLE INFO

Article history:
Received 4 February 2014
Received in revised form 14 April 2014
Accepted 15 April 2014
Available online 26 April 2014

Keywords:
HNP-1 variants
Arginine modified side chains
Bacterial model membrane
Reduced lipid–protein interaction
Spectroscopic techniques

ABSTRACT

α-Defensins (e.g. human neutrophil peptides, HNPs) have a broad spectrum bactericidal activity contributing to human innate immunity. The positive charge of amino acid side chains is responsible for the first interaction of cationic antimicrobial peptides with negatively charged bacterial membranes. α-Defensins contain a high content of Arg residues compared to Lys. In this paper, different peptide analogs including substitution of Arg-14 respectively with N^G–$N^{G'}$-asymmetric dimethyl-L-arginine (ADMA), N^G–$N^{G'}$-symmetric dimethyl-L-arginine (SDMA) and Lys (R14K and R15K) variants have been studied to test the role of Arg guanidino group and the localized cationic charge of Lys for interaction with lipid membranes. Our findings show that all the variants have a decreased disruptive activity against the bilayer. The methylated analogs show a reduction in membrane partitioning due to the lack of their ability to form hydrogen bonds. Comparison with the native HNP-1 peptide has been discussed.

Abbreviations: AMP, antimicrobial peptide; HNP-1, human neutrophil peptide 1; ADP, adenosine diphosphate; PMRTs, protein arginine methyltransferases; ADMA, N^G–$N^{G'}$-asymmetric dimethyl-L-arginine; SDMA, N^G–$N^{G'}$-symmetric dimethyl-L-arginine; MMA, N^G-monomethyl-L-arginine; POPG, 1-palmitoyl-2oleoyl-*sn*-glycerol-3-phosphoglycerol; POPE, 1-palmitoyl-2oleoyl-*sn*-glycerol-3-phosphoethanolamine; CL, 1,1′,2,2′-tetramyristoyl cardiolipin ammonium salt; PCSL, 1-acyl-2-[*n*-(4,4dimethyloxazolidinyl-N-oxyl)]stearoyl-*sn*-glycero-3-phosphocholine; MOPS, 3-(N-morpholino) propanesulfonic acid; LUVs, large unilamellar vesicles; CD, circular dichroism; EPR, electron paramagnetic resonance; PC, phopshatidylcholine.

* Corresponding author at: Department of Biotechnology, Chemistry and Pharmacy, University of Siena, Via A. Moro 2, 53100 Siena, Italy. Tel.: +39 0577 234258; fax: +39 0577 234239.
E-mail address: rebecca.pogni@unisi.it (R. Pogni).

http://dx.doi.org/10.1016/j.bpc.2014.04.003
0301-4622/

1. Introduction

Antimicrobial peptides (AMPs) have been isolated from plants, invertebrates, fish, insects, amphibians and mammals and constitute the first line of defense against bacteria and viruses [1,2]. The antimicrobial activity of some AMPs is based on membrane partitioning with phospholipid destabilization and pore formation, while other AMPs can inhibit more specific cellular targets such as protein expression and DNA replication [3,4]. Besides the composition of the phospholipid bilayer, the main factors that influence peptide–lipid interactions are the cationicity and the presence of hydrophobic residues in the peptide sequence [5].

Human neutrophil peptide 1 (HNP-1) is one of the most common human AMPs, expressed in the azurophil granules of neutrophils [6]. HNP-1 belongs to the class of α-defensin and it is structured in three β-sheets with three intramolecular disulfide bonds and a single β-hairpin. This peptide presents a total positive charge equal to +3 conferred by cationic arginines (Arg-5, Arg-14, Arg-15 and Arg-24) and anionic glutamic acid (Glu-13) [7,8]. Defensins are widely known to kill bacteria through electrostatic interactions with negatively-charged membranes. Arg residues are the most important for membrane interactions as the positively-charged side chains of cationic guanidino groups provide the initial long-range electrostatic attractive forces that guide the antimicrobial peptide toward the negatively-charged bacterial membranes. Arginines can also make electrostatic interactions with other residues (H-bonds, salt bridges and cationic–π contacts) important for structural stability [9,10].

In some inflammation diseases defensins can present an ADP-ribose unit linked to arginine residues that makes them inactive against pathogens. HNP-1 is ADP-ribosylated principally at Arg-14, which can be converted once modified, into an ornithine residue following a non-enzymatic hydrolytic reaction [11–13]. This post-translational modification to the guanidino group of arginine induces a reduction of peptide cationic charge. Along with ADP-ribosylation, also arginine methylation, catalyzed by a family of enzymes called protein arginine methyltransferases (PRMTs), represents another important protein post-translational modification. The change of arginine side chain guanidino groups is quantitatively one of the most extensive protein methylation reactions in mammalian cells [14]. Arginine is unique among amino acids as its guanidino group contains five potential hydrogen bond donors that are positioned for favorable interactions with biological hydrogen bond acceptors [15,16]. Thus, arginine modifications in proteins can readily modulate their binding interactions and thus regulate their physiological functions. The most prevalent methylated residue is N^G–$N^{G'}$-asymmetric dimethyl-L-arginine (ADMA), where two methyl groups are placed on one of the terminal nitrogen atoms of the guanidino group. Two other derivatives are formed, including the N^G–$N^{G'}$-symmetric dimethyl-L-arginine (SDMA) where one methyl group is placed on each of the terminal guanidino nitrogens and the mono-methylated derivative with a single methyl group on the terminal nitrogen atom, N^G-monomethyl-L-arginine (MMA) [15].

In this paper three different variants, including substitution of Arg-14 respectively with N^G–$N^{G'}$-asymmetric dimethyl-L-arginine (ADMA), N^G–$N^{G'}$-symmetric dimethyl-L-arginine (SDMA) and L-lysine (R14K) plus another variant replacing the Arg-15 with a L-lysine (R15K) have been studied for their interactions with lipid membranes. Although Arg and Lys have equivalent electropositive charges at neutral pH, only the Arg residues are thought to give selectivity to the peptides for preferential interactions with negatively charged bacterial membranes [16].

In this work, a biophysical study has been carried out to test the relevance of the dimethylated arginine residues (ADMA and SDMA) and lysine, incorporated into the most important sites of HNP-1, for partitioning into lipid membranes. All variants showed an altered capability of partition into lipid bilayer.

2. Material and methods

The dimethylated arginines (ADMA and SDMA) and lysine (R14K and R15K) peptide analogs of HNP-1 (Fig. 1) were obtained from Bachem (Bubendorf, CH) and used without further purification. All the variants used in the present study possess the same folding of native HNP-1 as confirmed by the Bachem data sheets.

The phospholipids for vesicle preparation, 1-palmitoyl-2oleoyl-*sn*-glycerol-3-phosphoglycerol (POPG), 1-palmitoyl-2oleoyl-*sn*-glycerol-3-phosphoethanolamine (POPE), 1,1′,2,2′-tetramyristoyl cardiolipin ammonium salt (CL), and spin-labeled phosphatidylcholine (1-acyl-2-[*n*-(4,4dimethyloxazolidinyl-N-oxyl)]stearoyl-*sn*-glycero-3-phosphocholine, *n*-PCSL, with n = 5, 7, 12) were obtained from Avanti Polar Lipids (Alabaster, AL). The buffer solution (pH 6.8) used in the experiments contains 50 mM of 3-(N-morpholino) propanesulfonic acid (MOPS) (Sigma Aldrich). MOPS is a buffer largely used for biological sample preparation due to its low salt content [17].

2.1. Liposome preparation

Liposomes were prepared by mixing 14 mM POPE, 12.9 mM POPG and 6.6 mM CL (POPE:POPG:CL 70:25:5 molar ratio), in agreement with the composition of lipids of Gram-negative bacterial inner membrane [18,19].

Lipids at the desired molar ratio dried down from chloroform stock solutions under a stream of nitrogen gas were then dried under vacuum for 1 h. The resulting lipid film was hydrated by adding 50 mM MOPS at pH 6.8 to reach a final concentration of about 50 mM phospholipids. Large unilamellar vesicles (LUVs) were prepared by freeze–thawing this lipid suspension five times followed by extrusion through 200 nm polycarbonate membrane filters using a Mini-Extruder syringe device (Avanti Polar Lipids). Final concentration of LUVs was determined using the Stewart phospholipids assay [20]. LUVs containing 1 mol of 5, 7, or 12-PCSL were prepared as described above. Different peptide:lipid molar ratios were prepared (1:250, 1:50, 1:30, 1:20, 1:15, 1:10 and 1:5) incubating each HNP-1 variant with LUVs in 50 mM MOPS buffer at pH 6.8 for at least 1 h.

2.2. Circular dichroism spectroscopy

Circular dichroism (CD) experiments were performed at room temperature on a Jasco CD-J-815 spectropolarimeter using a quartz cuvette with a path length of 1 mm. Peptides were suspended at 0.02 mM concentration in 50 mM MOPS at pH 6.8 with a constant or variable concentration of LUVs ranging from 0.1 to 5 mM. CD spectra were recorded from 190 to 250 nm and accumulated ten times to improve the signal-to-noise ratio. Baselines of either solvent or vesicular suspension without peptide were subtracted from each respective sample to calculate the peptide contribution [21].

2.3. Electron paramagnetic resonance spectroscopy

Electron paramagnetic resonance spectroscopy (EPR) spectra were recorded on a Bruker E500 ELEXSYS X-Band spectrometer equipped with a super-high-Q cavity at 303 K. Samples prepared for EPR measurements contained 0.4 mM of *n*-PCSL LUVs and a variable concentration of peptide ranging from 0.02 to 0.08 mM. Spectra were recorded using the following instrumental settings: 120 G sweep width; 100 kHz modulation frequency; 1.0 G modulation

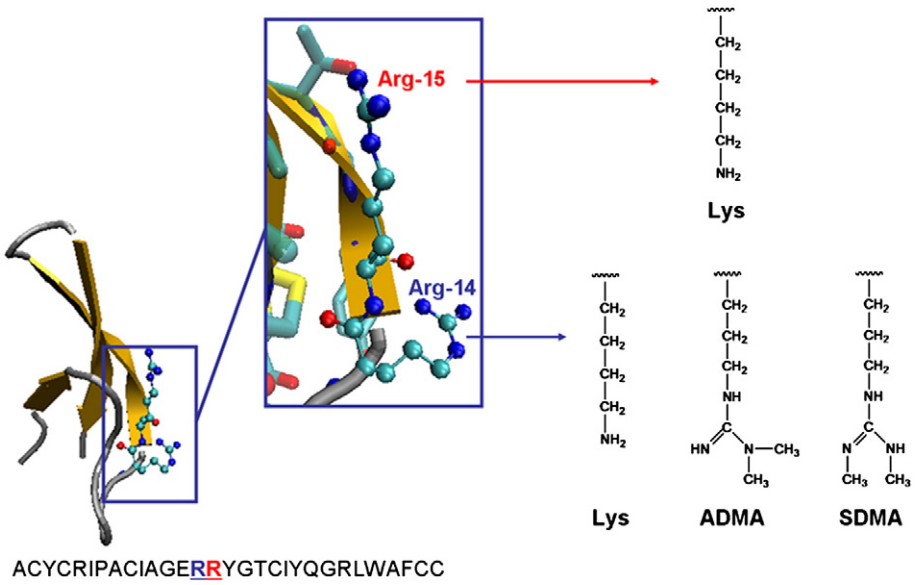

Fig. 1. Sequence and secondary structure of HNP-1 with Arg-14 (*blue*) and Arg-15 (*red*) highlighted. Side chain of the two forms of dimethylated residue and L-lysine is shown in correspondence of the specific replaced arginine. Peptide structure is taken from Protein Data Bank (*3GNY*) and the figure is obtained using Visual Molecular Dynamics software.

amplitude; 40 ms time constant; at 20 mW microwave power. Several scans, generally 15, were made to improve the signal-to-noise ratio. Values of the outer hyperfine coupling constant, $2A_{max}$, were determined by measuring the difference between the peaks at low and high field. Measurements were performed in triplicate and the reproducibility of $2A_{max}$ is typically ± 0.03–0.08 G. The relative values of $2\Delta A_{max}$ were obtained by calculating the difference of outer hyperfine coupling constant for the spectra with or without HNP-1 variants. To assess the rotational mobility of 12-PCSL (as reported in the following figure), the apparent rotational correlation time (τ) was determined according to Ref. [18]:

$$\tau = \left(0.65 \cdot 10^{-9}\right) \Delta H_0 \left[\left(A_0/A_{-1}\right)^{1/2} - 1\right] \quad (1)$$

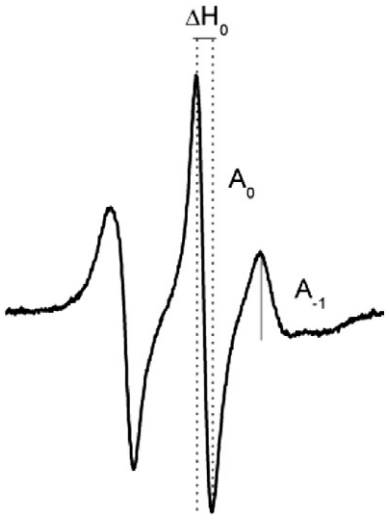

where ΔH_0 is the peak-to-peak width of the center line in gauss, A_0 is the amplitude of the center line, and A_{-1} is the amplitude of the high field line. The rotational correlation time is inversely related to the motional spin label rate such that an increase in τ indicates slower motion.

2.4. Fluorescence and thermodynamic measurements

Peptide–lipid interactions were studied by monitoring the change in the Trp-26 fluorescence emission spectra in the presence of LUVs. Samples prepared for fluorescence measurements contained 0.02 mM peptide and a variable phospholipids concentration ranging from 0.1 to 5 mM. Fluorescence measurements were performed on a Jasco FB-6500 spectrometer. The excitation wavelength was 280 nm, and emission spectra were recorded between 300 and 400 nm, with a 1 nm slit widths at room temperature [22,23]. A very small emission band in the range of 300–310 nm due to tyrosine residues contribution is present in some samples, but it does not influence the tryptophan fluorescence band [24].

Binding experiments of peptide to LUVs (0.02 mM HNP-1 variants in 50 mM MOPS buffer at pH 6.8) were performed with an ultrafiltration assay to separate lipid phase from the free peptide using Centricon-30 kDa cut-off filters (Millipore Inc.). Peptides were added to LUVs at a peptide:lipid molar ratios of 1:250, 1:50, 1:30, 1:20, 1:15, 1:10, and 1:5, incubated for 30 min and then centrifuged at 6000 ×g for 1 h [25].

The free peptide concentrations in the eluate have been determined through a calibration curve plotting known peptide concentration, vs. fluorescence intensity. The amount of the peptide bound to lipid was measured by subtracting the free peptide concentration from the total peptide concentration. Based on our CD studies, we found that α-defensin forms aggregates in solution at physiological pH at a concentration above 0.04 mM (data not shown). In all partition coefficient experiments, peptide concentration is maintained below 0.04 mM to avoid peptide aggregation process that could bring misleading interpretation of the data.

The mole fraction partition coefficient (K_p) was determined as following:

$$K_p = \left([P]_{bilayer}/[L]\right)/\left([P]_{wat}/[W]\right) \quad (2)$$

where [P] is the peptide concentration in the bilayer or water phase, [L] is the molar lipid concentration and [W] is the water molar concentration (55 mM at 25 °C) [26].

For quenching experiments samples were prepared in 50 mM MOPS (pH = 6.8) at a final peptide concentration of 0.02 mM. Vesicles were added in specific peptide:lipid molar ratios equal to 1:250, 1:20 and 1:5. After an incubation time of about 30 min, 2 mM potassium iodide (KI) was added and fluorescence spectra were recorded.

For doxyl-PCSL quenching experiments, spin labeled LUVs were prepared with the same protocol of the EPR spectroscopic analysis (see Material and methods, Electron paramagnetic resonance spectroscopy section). *n*-PCSL-LUVs were added to a solution containing 0.02 mM HNP-1 in 50 mM MOPS (pH = 6.8) to give 1:250, 1:20 and 1:5 peptide:lipid molar ratios, respectively. Each sample was incubated at room temperature for almost 30 min and fluorescence emission spectra were recorded before and after the incubation time as described [27,28]. For both analyses, quenching effect was calculated as the ratio between the intensity of fluorescence spectra in the presence and in the absence of the quencher (i.e. KI or doxyl-radical) for each specific peptide:lipid ratio. Fluorescence spectra were recorded with Jasco FB-6500 spectrometer using the same setting as previously described.

3. Results

3.1. Analysis on variants secondary structure

CD spectroscopy has been used to characterize the secondary structure of the peptides in solution and in the presence of POPE:POPG:CL membrane at different peptide:lipid molar ratios. In Fig. 2A the CD spectra of ADMA have been reported. In solution (Fig. 2A *black*) the ADMA peptide shows a negative peak at ~210 nm typical of a β-sheet structure with a lower part of unordered peptide. This spectrum differs from that reported previously for native HNP-1 [29], demonstrating that the replacement of Arg-14 with asymmetric dimethylated Arg influences the β-turn structure of the peptide. For 1:250 peptide:lipid molar ratio (Fig. 2A *green*) the CD spectrum has a negative peak at 205 nm assuming a line shape similar to a β-hairpin conformation. Reaching the 1:20 ratio (Fig. 2A *blue*) a negative peak at 208 nm, due to a β-sheet organization is evident [30]. For the 1:5 peptide:lipid ratio (Fig. 2A *red*) the CD spectrum essentially reflects a β-sheet structure.

In Fig. 2B the CD spectra for SDMA variant in solution and in the presence of model membranes (1:250, 1:20 and 1:5) have been reported. The replacement of arginine 14 with symmetric dimethyl guanidino group gives similar results as previously discussed for the ADMA variant.

CD spectra for R14K variant are reported in Fig. 2C. The free peptide in solution shows a minimum at ~205 nm indicating the presence of a β-hairpin structure and some percentage of α-helix conformation [31]. The spectrum resembles that obtained for native HNP-1 in solution [29]. For lower peptide:lipid molar ratio (1:250, Fig. 2C *green*) an increase in molar ellipticity and β-sheet structure is observed paired with the disappearance of α-helix contribution. When the 1:20 ratio (Fig. 2C *blue*) is reached, a negative peak at ~209 nm and a line shape close to a β-sheet structure are recorded. For 1:5 peptide:lipid ratio (Fig. 2C *red*) the presence of an α-helix contribution is evident and the spectrum is similar to that reported for the peptide in solution.

The CD spectra reported for the R15K variant show a negative peak at ~205 nm (β-hairpin) and a more pronounced percentage of α-helix contribution compared to the other variants (Fig. 2D). There are no significant variations in the spectra line shape for all the analyzed ratios.

3.2. Analysis of membrane–peptide interaction through emission fluorescence spectroscopy

The fluorescence emission spectra of the four variants have been used to follow the interaction of the peptides with POPE:POPG:CL vesicles. The variation in quantum yield and the shift in the emission maximum are typical of a tryptophan when it moves from an aqueous to a lipid environment. In our previous study, we have reported a clear blue shift and an increase in fluorescence quantum yield of the Trp-26 when native HNP-1 penetrates into the lipid bilayer at the threshold concentration (1:20 peptide:lipid molar ratio) [29].

Here the Trp fluorescence spectra for all variants in solution show the classical emission band at ~343 nm (Fig. 3). By adding liposomes for ADMA and SDMA a decrease in fluorescence quantum yield is observed in both cases for all the peptide:lipid molar ratios. Moreover, the fluorescence spectra show an unusual double peak at 332 nm and 352 nm, most probably reflecting two different orientations of Trp-26 upon interaction with lipid bilayer.

Fig. 3 (panels C and D) shows the fluorescence emission spectra of R14K and R15K variants respectively. In the presence of membranes with the 1:250 peptide:lipid molar ratio a strong decrease in quantum yield and a red shift to ~349 nm is detected. For higher ratios (1:20 and 1:5), a different trend is reported with a blue shift of the band (332 nm) revealing that Trp is translocated into the apolar environment of the bilayer [22,23,29]. Around 305 nm the fluorescence contribution of tyrosines is evident.

3.3. Determination of the depth of peptide insertion by Trp quenching

To evaluate the depth of peptides' penetration into the lipid bilayer, quenching experiments were performed. The measurements were done using doxyl labeled lipids as a membrane-bound depth dependent quencher. The doxyl group was anchored at positions 5, 7 or 12 of a stearoyl chain of PC lipid into the bilayer. On the other hand the potassium iodide (KI) quencher is used to estimate the water exposed indole moiety of tryptophan. Each value of emission quenching was calculated as the ratio between Trp fluorescence intensity in the presence and in the absence of doxyl labeled lipids or iodide [25].

In Table 1 the quenching values for each variants at three different peptide:lipid molar ratios in the presence of doxyl-lipid and potassium iodide are reported. For lower ratio (1:250 peptide:lipid) all the tested peptides show the highest value of quenching in the presence of KI leading to a massive exposition of Trp-26 to buffer. Nevertheless, a weak Trp quenching is reported exclusively for the nitroxide radical on position 5 of PC. Increasing peptide concentration (1:20 peptide:lipid molar ratio which represents the threshold concentration for native HNP-1) the ADMA and SDMA fluorescence emissions are well quenched by 5-doxyl and KI indicating a partial partition of Trp into the bilayer. Results are in agreement with fluorescence spectra where double peaks (332 nm and 352 nm) were recorded.

For R14K and R15K peptides at 1:20 peptide:lipid molar ratio, a deeper penetration into the bilayer is evident compared to ADMA and SDMA. This is particularly evident for the R15K variant. The experiments with KI confirm the same trend.

For 1:5 peptide:lipid molar ratio ADMA, SDMA and R14K are basically located on the external layer of membranes with Trp partially exposed to aqueous phase, as both 5-doxyl and KI present almost the same value of quenching. Indeed R15K variant shows an interaction also with 7-doxyl evidencing a deeper lipid destabilization.

3.4. Analysis of peptide–membrane interaction by EPR measurements

The EPR technique has been shown to be a useful tool to analyze the penetration of peptides into lipid vesicles using site-specific spin-labeled lipids. To determine the lipid penetration of HNP-1 variants, the motion of phosphatidylcholine spin labeled with nitroxide radicals positioned at different depths of alkyl chain has been examined. The changes in outer hyperfine coupling constant ($2A_{max}$) reflect the selectivity of interaction with lipid head-groups and also the different strengths of lipid interaction with peptides (see Fig. 4 *inset*) [31–34].

Fig. 4 shows the difference in outer hyperfine coupling constant of 5-PCSL in presence and absence of each variant ($2\Delta A_{max}$) at various peptide:lipid molar ratios (values of $2\Delta A_{max}$ are given in Table 2). Adding peptides in solution a linear increase in $2\Delta A_{max}$ is observable

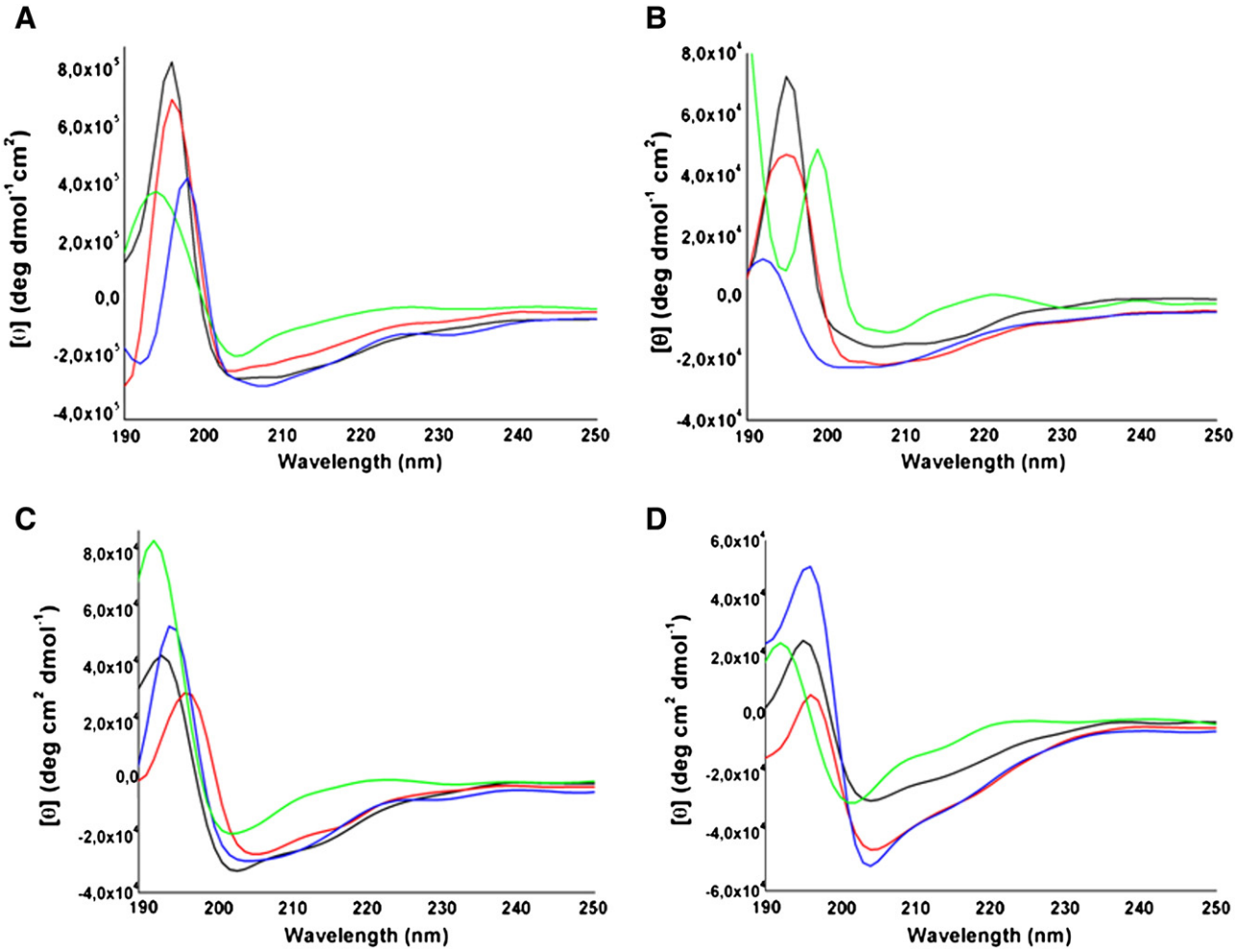

Fig. 2. Circular dichroism spectra (190–250 nm range) of ADMA (A), SDMA (B), R14K (C) and R15K (D) variants of HNP-1 peptide in 50 mM of MOPS buffer (pH 6.8) (*black*) and in presence of LUVs at peptide:lipid molar ratios of 1:250 (*green*), 1:20 (*blue*) and 1:5 (*red*) are reported. Baselines of either solvent or vesicular suspension without peptide have been subtracted from each sample. Spectral distortion is present below 195 nm due to liposome dispersion. Data are representative of three different experiments.

for ADMA, SDMA and R14K (Fig. 4 *circles*, *squares* and *up triangles* respectively), indicating a lipid perturbation on the outer part of membrane principally for 1:10 and 1:5 peptide:lipid molar ratios. R15K has a different behavior (Fig. 4 *down triangles*): for 1:30 and 1:15 ratios, $2\Delta A_{max}$ is basically similar to the other variants, but for 1:10 and 1:5 ratios a 60% higher difference in coupling constant compared to the others is revealed. This result shows that R15K for high ratios perturbs strongly the outer part of the lipid bilayer.

A similar trend in $2\Delta A_{max}$ for 7-PCSL of ADMA, SDMA and R14K is observed (Fig. 5 *circles*, *squares* and *up triangles* respectively), even if the magnitude of interaction results is smaller with respect to 5-PCSL. Instead, for R15K variant the 1:10 peptide:lipid ratio shows the highest value due to a deeper penetration into lipid bilayer (Fig. 5 *down triangles*).

For 12-PCSL (see Table 3), no particular changes in correlation time have been observed for ADMA, SDMA and R14K at all ratios. Only R15K produce an increase on τ for 1:20 peptide:lipid ratio indicating a peptide localization into the hydrophobic core of membranes.

3.5. Peptide–membrane partitioning

The variants partition coefficient values have been obtained using fluorescence emission technique (see Eq. (2) in Material and methods). K_P allows estimation of the partition capability of peptides into the lipid bilayer at different molar ratios [26].

In Fig. 6 the partition coefficients of the variants have been reported and compared to those obtained for the native HNP-1 [29]. At 1:250 peptide:lipid molar ratio the lower values of membrane partitioning have been recorded. By increasing the peptide:lipid molar ratio for ADMA and SDMA a weak interaction with lipid bilayer is discernible. The highest K_P values for both variants are reported for 1:5 and 1:10 ratios (see Table 4). R14K and R15K show the higher values of K_P for 1:20 ratio. The trend is similar to that detected for the native peptide even if with a strong reduction of lipid destabilization [29].

4. Discussion

In α-defensins there is a selection of arginine over lysine residues. It is widely reported that Arg is a better residue than Lys in killing bacteria and this is more evident in α-defensins than in β-defensins [35]. Arg and Lys are both polar residues possessing side chains that are amphiphilic in nature, with a positively charged guanidino (pKa = 11–13) or amino group (pKa = 9–10) respectively. Furthermore, side chain interactions of Arg mainly involve the guanidino group, whereas Lys has contacts with other residues through both its methylene and amino groups [36,37]. The enhanced capacity of Arg for electrostatic interactions appears to stem from the delocalized cationic charge over the guanidino group versus a more localized cationic charge for Lys. Furthermore, guanidino group is capable of forming more extensive and stronger H-bonds with other donors and/or acceptor [9,16]. This may

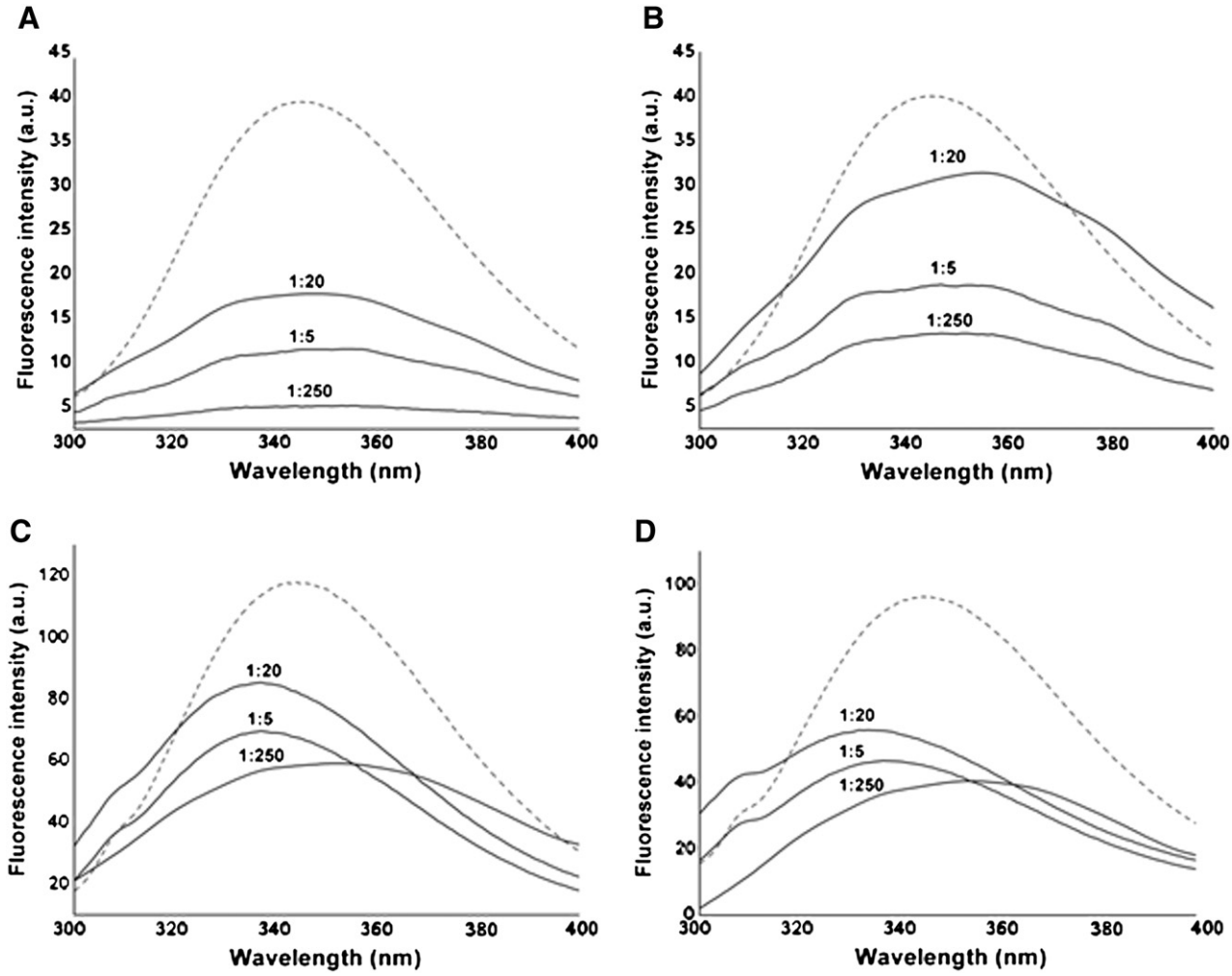

Fig. 3. Tryptophan emission spectra (range 300–400 nm) of ADMA (A), SDMA (B), R14K (C) and R15K (D) in MOPS buffer (*dotted line*) and in presence of LUVs at peptide:lipid molar ratios of 1:250, 1:20 and 1:5 are reported. The excitation wavelength was 280 nm. The spectra were recorded at room temperature. Band around 310 nm is due to tyrosine contribution. Spectra have been collected three times.

explain why Arg is a better cationic residue than Lys in the electrostatic force mediated killing of bacteria by defensins. Considering also that arginine guanidino group is one of the principal sites for methylation reactions in mammalian cells, four variants at positions 14 or 15 have been studied and their partition into negatively charged lipid membranes have been analyzed. Each addition of methyl groups in arginine-dimethylated variants, asymmetric dimethyl arginine (ADMA) and symmetric dimethyl arginine (SDMA) of HNP-1 not only changes its shape, but also removes potential hydrogen bond donors. R14K and R15K peptide analogs of HNP-1 have been characterized to test the role of these sites versus Arg in the partition into lipid bilayers. Recently in a paper published by our group, the interaction of HNP-1 with model membranes mimicking the composition of Gram-negative bacteria inner membrane at different peptide:lipid molar ratios has been studied [29]. The partitioning of native defensin in lipid membranes changes with increasing peptide concentration. The 1:20 peptide:lipid molar ratio was identified as the threshold concentration for the penetration of peptide into the lipid bilayer. The same type of approach has been performed here in order to assess the effect of Arg modified residues on the interaction with lipid bilayer. The CD spectra for all the variants show little variation in their secondary structure compared to the native peptide. The greatest variations are reported for the SDMA and ADMA peptide analogs in solution as the methylation of Arg 14 influences the β-turn structure. For interaction with lipid membranes, at 1:20 peptide:lipid molar ratio, a more clear β-sheet structure is assumed by

Table 1
Measurements of tryptophan fluorescence quenching calculated for ADMA, SDMA, R14K and R15K variants at 1:250, 1:20 and 1:5 peptide:lipid molar ratios.

Peptide	5[b]-doxyl PCSL	7[b]-doxyl PCSL	12[b]-doxyl PCSL	KI[a]
1:250 pep:lip				
ADMA	0.81	/	/	0.21
SDMA	0.77	/	/	0.27
R14K	0.79	/	/	0.22
R15K	0.85	/	/	0.33
1:20 pep:lip				
ADMA	0.68	0.78	0.98	0.34
SDMA	0.61	0.86	0.93	0.31
R14K	0.56	0.63	0.88	0.54
R15K	0.51	0.58	0.65	0.62
1:5 pep:lip				
ADMA	0.53	0.78	0.96	0.45
SDMA	0.48	0.86	0.97	0.41
R14K	0.62	0.63	0.84	0.34
R15K	0.59	0.58	0.87	0.38

Fluorescence maximum intensity is recorded in the 330–340 nm range. Quenching is calculated as ratio between the fluorescence intensity in presence and absence of quencher for each peptide:lipid molar ratio.

[a] KI quencher is used to determine water exposed Trp residue with LUVs in solution.

[b] The doxyl-labeled lipid quenches Trp fluorescence in a distance dependent manner, giving the depth of penetration of peptide into vesicles.

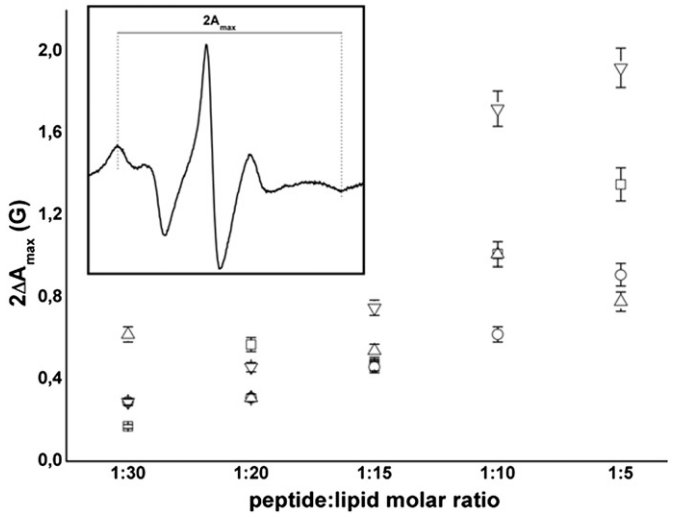

Fig. 4. Difference in the outer hyperfine coupling constants ($2\Delta A_{max}$) of 5-PCSL for different peptide:lipid ratios calculated for ADMA (*circles*), SDMA (*squares*), R14K (*up triangles*) and R15K (*down triangles*) variants. Error bars indicate standard deviations from at least three independent measurements (*inset*) CW-EPR spectra of 5-PCSL recorded with (*upper spectrum*) and without (*lower spectrum*) ADMA are reported as an example. T = 303 K, 120 G scan widths, 1.0 G modulation amplitude, $\nu = 9.86$ GHz.

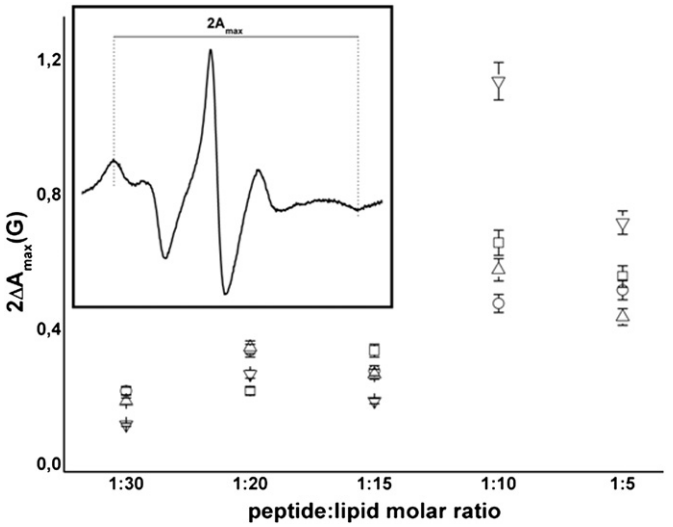

Fig. 5. Difference in the outer hyperfine coupling constants ($2\Delta A_{max}$) of 7-PCSL for different peptide:lipid ratios calculated for ADMA (*circles*), SDMA (*squares*), R14K (*up triangles*) and R15K (*down triangles*) peptides. Error bars indicate standard deviations from at least three different measurements. (*inset*) CW-EPR spectra of 7-PCSL recorded with (*upper spectrum*) and without (*lower spectrum*) ADMA are reported as an example. T = 303 K, 120 G scan widths, 1.0 G modulation amplitude, $\nu = 9.86$ GHz.

both variants and it has been calculated to be approximately 67%, compared to the native peptide which presents 41% beta-sheet structure. For R14K and R15K variants the secondary structure in solution and in presence of membranes resembles that previously recorded for the native peptide.

This shows that the modifications introduced into the variants structure do not influence to a great extent the secondary structure of the proteins.

On the other hand, marked differences in variants partitioning compared to the native HNP-1 have been detected when the emission fluorescence spectra are recorded.

The wavelength of maximum emission of the Trp for all the variants in solution was around 343 nm [29]. The interesting aspect is that in the presence of lipid bilayer the quantum yield is well below that recorded for the peptides free in solution for all the ratios. This aspect could indicate peptide aggregation for the increase in hydrophobicity due the methylation of guanidino group for all the tested peptide:lipid molar ratios. In the case of the ADMA and SDMA variants the presence of two peaks at ~332 nm and ~350 nm suggest an interfacial location of the Trp residue. The same trend recorded for both variants shows that the different shape (asymmetric and symmetric) does not influence the interaction with lipid bilayer but in both cases the Trp residue is localized in the interfacial region of the lipid bilayer. It is exposed to lipids and water simultaneously. The Trp maximum emission band is quite sensitive to its local environment, ranging from ~308 nm to ~355 nm and roughly correlates with the degree of solvent exposure of the chromophore. Quantum mechanical studies, taking into account the full solvation of different protein environments, have reproduced the Trp emission wavelength in several proteins showing that the red or blue shift can be related to a different exposure of the faces and edge of Trp residue [38–40]. In our case different orientation of the solvent exposed Trp has been monitored at the same time. The two variants have shown a significant KI quenching (see Table 1) for the 1:250 peptide to lipid molar ratio. This quenching was slightly increased for higher ratios but in all cases the peptide is confined to the external leaflet of the bilayer also for the 1:20 peptide:lipid molar ratio, which represents the threshold concentration for the native peptide.

For a more localized charge, as for the R14K and R15K variants, the interaction with the bilayer is significantly decreased compared to HNP-1. In these cases the fluorescence spectra show a blue shift of the fluorescence emission band to 332 nm for the 1:20 and 1:5 molar ratios indicating the translocation of the peptides to the apolar environments without penetration [22,23,29]. The KI quenching experiments show a better partitioning in the bilayer in respect to ADMA and SDMA but not a real insertion. The R15K variant partitioning into the bilayer is more evident than for R14K showing a more relevant role of the latter

Table 2
Values of $2\Delta A_{max}$ (G) calculated for all HNP-1 variants at different peptide:lipid molar ratios.

5-PCSL				
Pep:lip	[a]ADMA ± 0.05 G	[a]SDMA ± 0.07 G	[a]R14K ± 0.07 G	[a]R15K ± 0.04 G
1:30	0.17	0.29	0.31	0.29
1:20	0.57	0.31	0.62	0.46
1:15	0.47	0.46	0.54	0.75
1:10	1.01	0.62	1.01	1.72
1:5	1.35	0.91	0.78	1.92
7-PCSL				
Pep:lip	[b]ADMA ± 0.08 G	[b]SDMA ± 0.08 G	[b]R14K ± 0.05 G	[b]R15K ± 0.03 G
1:30	0.19	0.19	0.16	0.09
1:20	0.19	0.31	0.32	0.24
1:15	0.30	0.25	0.24	0.16
1:10	0.63	0.45	0.55	1.11
1:5	0.53	0.49	0.41	0.69

$2\Delta A_{max}$ has been calculated from difference in outer splitting constant of [a]5- and [b]7-PCSL in presence and absence of peptides. Standard deviations values (±) have been obtained from three independent EPR measurements. Spectra were collected at 303 K.

Table 3
Correlation times (τ) for 12-PCSL incorporated in LUVs as a function of peptide:lipid molar ratio calculated for ADMA, SDMA, R14K and R15K variants.

Pep:lip	ADMA (ns)	SDMA (ns)	R14K (ns)	R15K (ns)
0:1	3.17	3.17	3.17	3.17
1:30	3.13	3.13	3.15	3.17
1:20	3.16	3.12	3.20	3.37
1:15	3.19	3.12	3.14	3.14
1:10	3.14	3.18	3.18	3.22
1:5	3.13	3.21	3.17	3.20

Mean standard error (±0.07 ns) from three different experiments at 303 K is reported.

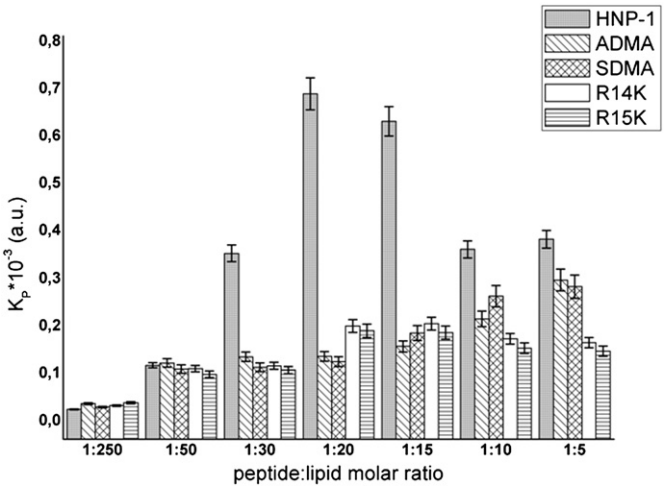

Fig. 6. Partition coefficients calculated at *low* (1:250 and 1:50) and *high* (1:30, 1:20, 1:15, 1:10 and 1:5) peptide:lipid molar ratios for ADMA, SDMA, R14K and R15K variants of HNP-1. K_P values for HNP-1 were taken from Bonucci et al. [29]. Error bars indicate standard deviation calculated from three independent measurements.

variant for the interaction with membranes. The EPR results are in agreement with all the other data showing the same trend for all the variants. The only significant variation in the EPR data is recorded for the R15K variant showing for high peptide concentration a more significant perturbation of the lipid bilayer (Tables 2 and 3).

Concerning the partition coefficient data (Fig. 6 and Table 4), the higher value was recorded for HNP-1 at the 1:20 molar ratio, the threshold concentration at which the peptide is inserted into the lipid bilayer, while at low (1:250) and higher peptide concentrations (1:5) it is localized on the surface with a different level of bilayer partitioning. In the case of the variants we cannot differentiate the partitioning once the peptide concentration is changed, for all the ratios the peptides are placed on the external leaflet of the membranes with no great variations. For ADMA and SDMA peptide analogs an increase in partition coefficient is detected at higher peptide:lipid molar ratio. This effect can be explained considering a cooperative increase in partitioning due to peptide aggregation on the membrane. The two peptides with methylated cationic residues (ADMA and SDMA) have decreased membrane permeability due to an increase in hydrophobicity and the loss of their capacity to form hydrogen bonds, even if the steric effects of methyl groups in substituted peptides may also contribute to decrease membrane interactions. These data show that the Arg14 residue is pivotal for the interaction of peptide with negatively charged membranes and its role for peptide lipid partition is dominant on that of Arg15 residue.

The replacement of Arg with Lys (R14K and R15K) in peptide sequence shows that for an efficient interaction and membrane disruptive properties the delocalized positive charge of the guanidino group in respect to a more cationic localized charge, is crucial paired with its ability to form hydrogen bonds. The role of arginine to form hydrogen bonds is unique. Guanidino group contains five potential hydrogen bond donors that are positioned for favorable interactions with biological hydrogen bond acceptors. Any variation to this group, changing its shape or charge, as occurring for post-translational modifications like addition of methyl or ADP-ribose groups, greatly interfere with membrane binding properties as demonstrated in this study.

Table 4
Partition coefficients values ($K_p \times 10^{-3}$) for ADMA, SDMA, R14K and R15K variants and HNP-1 peptide at various peptide:lipid molar ratios.

Pep:lip	HNP-1[a]	ADMA	SDMA	R14K	R15K
1:250	0.02	0.02	0.01	0.02	0.03
1:50	0.11	0.11	0.09	0.09	0.08
1:30	0.34	0.12	0.10	0.10	0.09
1:20	0.68	0.13	0.11	0.19	0.18
1:15	0.62	0.15	0.17	0.19	0.17
1:10	0.35	0.21	0.25	0.16	0.14
1:5	0.37	0.29	0.27	0.15	0.13

The range of maximum emission wavelength range for calculating free peptide in solution is 330–350 nm. Average standard deviation equal to ±8% is calculated from three different measurements in the same experimental conditions.

[a] Partition coefficient values for native HNP-1 were taken from Ref. [29]. Error on K_p (±5%) was obtained from three independent analysis.

5. Conclusions

In this paper, different variants on Arg residue 14 and 15 have been analyzed for interaction with negative charged lipid bilayer mimicking the inner membrane of Gram-negative bacteria. All the variants independently from the substitution on Arg14 have shown a marked reduction in lipid partitioning. The peptides are mainly localized on the outer leaflet of the membrane and no evident insertion into lipid bilayer has been detected. This shows that the electrostatic interaction is the driving force for the initial partitioning of the peptides into membranes paired with the unique ability of the Arg guanidino group to form hydrogen bonds. Furthermore, the peptide analogs with Lys residue (R14K and R15K) show a reduced membrane disruptive activity than the Arg guanidino group.

References

[1] R.E. Hancock, G. Diamond, The role of cationic antimicrobial peptides in innate host defence, Trends Microbiol. 8 (2000) 402–410.
[2] R.E. Hancock, R. Lehrer, Cationic peptides: a new source of antibiotics, Trends Biotechnol. 16 (1998) 82–88.
[3] H. Jessen, P. Hamill, R.E. Hancock, Peptide antimicrobial agent, Clin. Microbiol. Rev. 19 (2006) 491–511.
[4] K.A. Brogden, Antimicrobial peptides: pore formers or metabolic inhibitors in bacteria, Nat. Rev. 3 (2005) 238–250.
[5] M.R. Yeaman, N. Yount, Mechanism of antimicrobial peptide action and resistance, Pharmacol. Rev. 55 (2003) 27–55.
[6] R.I. Lehrer, Primate defensin, Nat. Rev. Microbiol. 2 (2004) 727–738.
[7] W. Zhibin, L. Xiangquen, E. de Leeuw, B. Ericksen, L. Wuyuan, Why is the Arg^5–Glu^{13} salt bridge conserved in mammalian α-defensins, J. Biol. Chem. 52 (2005) 43039–43047.
[8] M. Edith, T. Ganz, R.I. Lehrer, Defensins and other endogenous peptide antibiotics of invertebrates, J. Leukoc. Biol. 58 (1995) 128–136.
[9] D.I. Chan, E.J. Prenner, H.J. Vogel, Tryptophan- and arginine-rich antimicrobial peptides: structures and mechanisms of action, Biochim. Biophys. Acta Biomembr. 9 (2006) 1184–1202.
[10] M.P. Aliste, J.L. MacCallum, D.P. Tieleman, Molecular dynamics simulation of pentapeptides at interfaces: salt bridge and cation–π interactions, Biochemistry 42 (2003) 8976–8987.
[11] G. Paone, L.A. Stevens, R.L. Levine, ADP-ribosyltransferase-specific modification of human neutrophil peptide-1, J. Biol. Chem. 25 (2006) 17054–17060.
[12] G. Paone, A. Wada, L.A. Stevens, ADP ribosylation of human neutrophil peptide-1 regulates its biological properties, Proc. Natl. Acad. Sci. U. S. A. 12 (2002) 8231–8235.
[13] L.A. Stevens, R.L. Levine, B.R. Bernardette, J. Moss, ADP-ribosylation of human defensin HNP-1 results in the replacement of the modified arginine with the non coded amino acid ornithine, Proc. Natl. Acad. Sci. U. S. A. 106 (2009) 19796–19800.
[14] S. Pahlich, R.P. Zakaryan, H. Gehring, Protein arginine methylation: cellular functions and methods of analysis, Biochim. Biophys. Acta 1764 (2006) 1890–1903.
[15] M.T. Bedford, S.G. Clarke, Protein arginine methylation in mammals: who, what and why, Mol. Cell 33 (2009) 1–13.
[16] L.T. Nguyen, L. de Boer, S.A.J. Zaat, H.J. Vogel, Investigating the cationic side chains of the antimicrobial peptide tritrpticin: hydrogen bonding properties govern its membrane-disruptive activities, Biochim. Biophys. Acta Biomembr. 1808 (2011) 2297–2303.
[17] N.E. Good, G.D. Winget, W. Winter, T.N. Connolly, Hydrogen ion buffers for biological research, Biochemistry 5 (1966) 467–477.
[18] S. Pistolesi, R. Pogni, J.B. Feix, Membrane insertion and bilayer perturbation by antimicrobial peptide CM15, Biophys. J. 93 (2007) 1651–1660.
[19] S. Lopes, C.S. Neves, P. Eaton, P. Gameiro, Cardiolipin, a key component to mimic *E. coli* bacterial membrane in model system revealed by dynamic light scattering and steady-state fluorescence anisotropy, Anal. Bioanal. Chem. 398 (2010) 1357–1366.
[20] J.C.M. Stewart, Colorimetric determination of phospholipids with ammonium ferrothiocyanate, Anal. Biochem. 104 (1980) 10–14.
[21] W.T. Heller, A.J. Waring, R.I. Lehrer, H.W. Huang, Multiple states of β-sheet peptide protegrin in lipid bilayers, Biochemistry 37 (1998) 17331–17338.
[22] A.S. Ladokhin, S. Jayasinghe, S.H. White, How to measure and analyze tryptophan fluorescence in membrane properly, and why bother? Anal. Biochem. 285 (2000) 235–245.

[23] B. Christianes, S. Symoens, S. Vanderheyden, Y. Englborghs, A. Joliot, A. Prochiants, J. Vandekerckhove, M. Rosseneu, B. Vanloo, Tryptophan fluorescence study of the interaction of penetrating peptides with model membranes, Eur. J. Biochem. 269 (2002) 2918–2926.
[24] Y. Groemping, N. Hellmann, Spectroscopic methods for the determination of protein interaction, Curr. Protoc. Protein Sci. (2005), http://dx.doi.org/10.1002/0471140864.ps2008s39.
[25] S.H. White, W.C. Wimley, A.S. Ladokhin, K. Hristova, Protein folding in membranes: determining energetics of peptide–bilayer interactions, Methods Enzymol. 295 (1998) 62–87.
[26] D.A. Allende, A. Vidal, S.A. Simon, T.J. McIntosh, Bilayer interfacial properties modulate the binding of amphipathic peptides, Chem. Phys. Lipids 122 (2003) 65–76.
[27] J.M. Rausch, R.J. Marks, R. Rathinakamur, W.C. Wimley, β-Sheet pore-forming peptides selected from a rotational combinatory library: mechanism of pore formation in lipid vesicles, Biochemistry 46 (2007) 12124–12139.
[28] L.P. Liu, C.M. Deber, Anionic phospholipids modulate peptide insertion into membranes, Biochemistry 36 (1997) 5476–5482.
[29] A. Bonucci, E. Balducci, S. Pistolesi, R. Pogni, The defensin–lipid interaction: insights on the binding state of the human antimicrobial peptide HNP-1 to model bacterial membranes, Biochim. Biophys. Acta Biomembr. 1828 (2013) 758–764.
[30] D. Sun, Z. Ren, X. Zeng, Y. You, W. Pan, M. Zhou, L. Wang, A. Xu, Structure–function relationship of conotoxin lt14a, a potential analgesic with low cytotoxicity, Peptides 32 (2011) 300–305.
[31] G. D'Errico, A.M. D'Ursi, D. Marsh, Interaction of a peptide derived from glycoprotein gp36 of feline immunodeficiency virus and its liposylated analogue with phospholipid membranes, Biochemistry 47 (2008) 5317–5327.
[32] D. Marsh, Electron spin resonance in membrane research: protein–lipid interactions from challenging beginnings to state of the art, Eur. Biophys. J. 39 (2010) 513–525.
[33] E. Sevcsik, G. Pabst, W. Richter, S. Danner, H. Amenitsch, K. Lohner, Interaction of LL-37 with model membrane system of different complexity: influence of the lipid matrix, Biophys. J. 94 (2008) 4688–4699.
[34] A. Falanga, R. Tarallo, G. Vitiello, M. Vitiello, E. Perillo, M. Cantisani, G. D'Errico, M. Galdiero, S. Galdiero, Biophysical characterization and membrane interaction of two fusion loops of glycoprotein B from herpes simplex type I virus, PLoS One 7 (2012), http://dx.doi.org/10.1371/journal.pone.0032186.
[35] R.A. Llenado, C.S. Weeks, M.J. Cocco, A.J. Ouellette, Electropositive charge in α-defensin bactericidal activity: functional effects of lys-for-arg substitution vary with the peptide primary structure, Infect. Immun. 77 (2009) 5035–5043.
[36] Y. Nozaki, C. Tanford, The solubility of aminoacids, diglycine and triglycine in aqueous guanidine hydrochloride solutions, J. Biol. Chem. 246 (1971) 211–2217.
[37] P.A. Karplus, Hydrophobicity regained, Protein Sci. 6 (1997) 1302–1307.
[38] S. Pistolesi, A. Sinicropi, R. Pogni, R. Basosi, N. Ferrè, M. Olivucci, Modeling the fluorescence of protein-embedded tryptophans with ab initio multiconfigurational quantum chemistry: the limiting case of parvalbumin and monellin, J. Phys. Chem. 113 (2009) 16082–16090.
[39] C. Bernini, T. Andruniow, M. Olivucci, R. Pogni, R. Basosi, A. Sinicropi, Effects of protein environment on the spectral properties of tryptophan radicals in *Pseudomonas aeruginosa* Azurin, J. Am. Chem. Soc. 135 (2013) 4822–4833.
[40] J.T. Vivian, P.R. Cullis, Mechanism of tryptophan fluorescence shifts in protein, Biophys. J. 80 (2001) 2093–2109.